ELSEVIER

Catalysis Today 51 (1999) 469–479

CATALYSIS TODAY

Progress on the mechanistic understanding of SO_2 oxidation catalysts

O.B. Lapina[a], B.S. Bal'zhinimaev[a], S. Boghosian[b], K.M. Eriksen[c], R. Fehrmann[c,*]

[a]*Boreskov Institute of Catalysis, 630090, Novosibirsk, Russian Federation*
[b]*Department of Chemical Engineering, University of Patras and Institute of Chemical Engineering and High Temperature Chemical Processes (ICE/HT-FORTH), GR-26500, Patras, Greece*
[c]*Department of Chemistry, Technical University of Denmark, DK-2800, Lyngby, Denmark*

Abstract

For almost a century vanadium oxide based catalysts have been the dominant materials in industrial processes for sulfuric acid production. A vast body of information leading to fundamental knowledge on the catalytic process was obtained by Academician [G.K. Boreskov, Catalysis in Sulphuric Acid Production, Goskhimizdat (in Russian), Moscow, 1954, p. 348]. In recent years these catalysts have also been used to clean flue gases and other SO_2 containing industrial off-gases. In spite of the importance and long utilization of these industrial processes, the catalytic active species and the reaction mechanism have been virtually unknown until recent years.

It is now recognized that the working catalyst is well described by the molten salt/gas system $M_2S_2O_7$–$MHSO_4$–V_2O_5/SO_2–O_2–SO_3–H_2O–CO_2–N_2 (M=Na, K, Cs) at 400–600°C and that vanadium complexes play a key role in the catalytic reaction mechanism.

A multiinstrumental investigation that combine the efforts of four groups from four different countries has been carried out on the model system as well as on working industrial catalysts. Detailed information has been obtained on the complex and on the redox chemistry of vanadium. Based on this, a deeper understanding of the reaction mechanism has been achieved.

Keywords: Flue gases; Vanadium oxide; SO_2 oxidation; Reaction mechanism

1. Introduction

The catalyst used for sulfuric acid production catalyzing the reaction $2SO_2+O_2 \rightleftarrows 2SO_3$ is a supported liquid phase (SLP) catalyst, usually made by calcination of diatomaceous earth, vanadium pentoxide (or other V salts) and alkali salt promoters (usually in the form of sulfates) with an alkali-to-vanadium molar ratio ranging from 2 to 5. During the activation process, large quantities of sulfur oxides are taken up by the catalyst, forming molten alkali pyrosulfates [1–3] which dissolve the vanadium salts. The molten salt–gas system $M_2S_2O_7$–$MHSO_4$–V_2O_5/SO_2–O_2–SO_3–H_2O–CO_2–N_2 (M=Na, K, Cs) is thus considered to be a realistic model of the working industrial catalyst. A major problem in the SO_2 oxidation process is the sudden drop in activity which is experienced in all commercial catalysts at an operating temperature below 420°C. Interstage (and costly) absorption of SO_3 before the last catalyst bed has thus become unavoidable in order to attain low SO_2 content in the stack gas.

*Corresponding author.

0920-5861/99/$ – see front matter
PII: S0920-5861(99)00034-6

Previously [4,5] very little has been known about complex and compound formation in the catalyst. However, this fundamental knowledge is essential for an understanding of the reaction mechanism and of the severe deactivation of the catalyst below ~420°C. Unfortunately, a direct study of the species formed in the liquid phase, which is dispersed in the small pores of the industrial catalyst, is very difficult and probably only methods like ESR and NMR can be applied. Applications of magnetic resonance techniques to study vanadium catalysts have been initiated by Mastikhin et al. [6,7]. He was the first who directly showed that under reaction conditions, (i.e. at 400–500°C) the active component exists as a melt forming a very thin liquid layer on the surface of the support [8]. ESR spectra measured at temperatures up to 500°C revealed that precipitation of V(IV) compounds caused deactivation of the catalysts [9,10].

The present paper reviews an ongoing study dealing with (i) the complex and redox chemistry of vanadium; (ii) the formation of V(III), V(IV) and V(V) compounds; (iii) the physico-chemical properties of the catalyst model system [11–13]. The strategy is to study both the working industrial catalysts and model systems in order to check if their chemistries can be linked together. In addition to ESR and NMR spectroscopy, the study of the catalyst model system includes methods such as UV/Vis-, FTIR- and Raman spectroscopy, electrical conductivity, potentiometry, EXAFS, XRD, neutron diffraction, thermal analysis, differential enthalpic analysis and differential scanning calorimetry.

2. Experimental

Pure and dry $M_2S_2O_7$ (M=Na, K, Cs) were made by thermal decomposition of the corresponding peroxodisulfates as described earlier [11]. V_2O_5 was from Cerac (pure, >99%). The investigated catalysts were from Haldor Topsoe A/S, Denmark, Monsanto, USA and Russia, both commercial and prototype. The instrumentation, furnaces and glove boxes used have been described in detail elsewhere [13,14].

The experimental set-up for in situ ESR and catalytic activity measurements in unconverted and preconverted 10% SO_2, 11% O_2, 79% N_2 sulfuric acid synthesis gas or wet 0.2% SO_2, 4% O_2, 7% H_2O, 14.1% CO_2 and 74.8% N_2 and dry 0.2% SO_2, 4.5% O_2, 15.1% CO_2 and 80.2% N_2 power plant flue gases, is shown in Fig. 1. This set-up also allows the compounds formed during deactivation in catalyst model melts to be isolated by use of a molten salt reactor cell [11]. The salt is supported on a porous frit through which the gases are passed at the desired temperature up to 500°C. Alternatively, the gases are led to a JEOL-JES-ME 1X ESR spectrometer equipped with a Bruker ER 4114HT high temperature X-band cavity, a small quartz reactor flow cell containing the crushed catalyst pellets being placed in the cavity as described earlier [15].

Multinuclear NMR spectra were measured on a Bruker MSL-400 spectrometer with a magnetic field of 9.4 T and resonance frequencies tuned for the different nuclei [16]. High temperature NMR measurements were using a home-built cell [14]. Details concerning the sample handling and preparation are given elsewhere [16–18]. Sample equilibration was performed by heating at 450°C for up to 20 days before recording Raman spectra. This was necessary due to the slow dissolution of sulfate and the slow diffusion of SO_2 and SO_3. Raman spectra were excited with the 647.1 nm lines of a Spectra Physics Stabilite model 2017 Krypton laser or the 514.5 nm line of a Spectra Physics 164 Argon ion laser. The scattered light was collected at an angle of 90° (horizontal scattering plane) and analyzed with a Spex 1403, 0.85 m double monochromator equipped with a −20°C RCA photomultiplier and EG&G/ORTEC rate meter and photon counting electronics. The experimental set-up and the procedure followed for obtaining Raman spectra at elevated temperatures have been described earlier in detail [19]. It should be pointed out here that recording of the Raman spectra at elevated temperatures from these very dark-colored, viscous and hygroscopic melts has proven very difficult due to strong absorption of the incident exciting laser light.

3. Results and discussion

According to ^{51}V NMR measurements, the various catalysts become quite similar after treatment under reaction conditions. This indicates that the active component in these catalysts is the same and is actually formed during the course of the catalytic

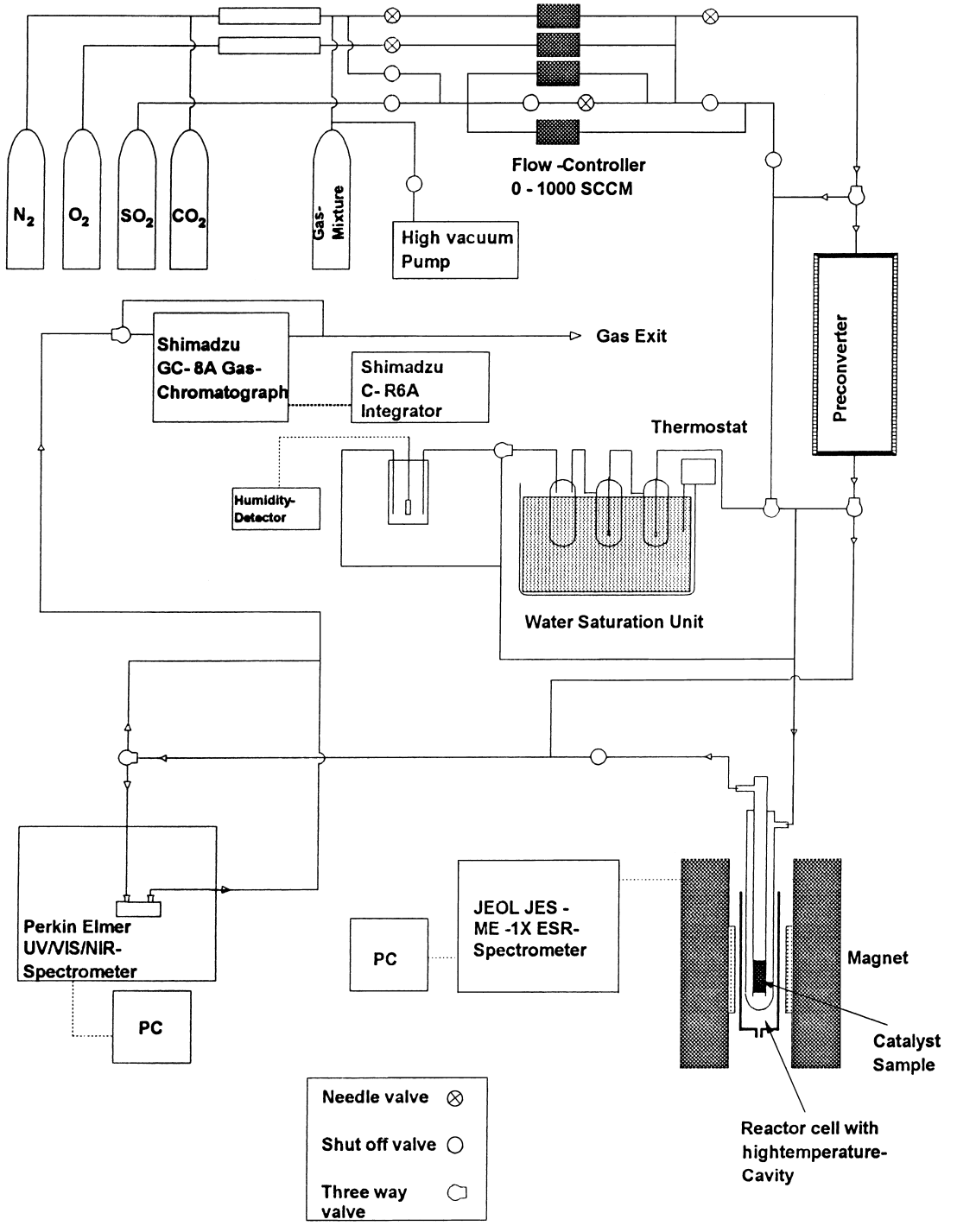

Fig. 1. Flow diagram for the experimental set-up for combined in situ ESR and activity investigations of SO_2 oxidation catalysts.

reaction. Initially, catalysts arising from different preparations contain a variety of V species. However, on interaction with the components of the reaction media, only two V species are formed. One of the species corresponds to V atoms in a slightly distorted tetrahedral coordination and can be attributed to vanadium bonded to the support. The second belongs to V atoms in distorted octahedral coordination typical for oxosulfatovanadates (V) (compounds formed between V_2O_5 and $M_2S_2O_7$).

Measurements of the catalytic activity has shown that tetrahedral vanadium species are inactive in SO_2 oxidation. To elucidate which V species are active in SO_2 oxidation, NMR spectroscopy was combined with catalytic activity measurements of the melts and of the catalysts. Thus, multinuclear ^{51}V, ^{23}Na, ^{39}K, ^{133}Cs and ^{17}O NMR studies of the V_2O_5–$M_2S_2O_7$ (M=K, Na, Cs) systems were carried out over the temperature range from 25°C to 500°C. The data obtained showed that the type of vanadium complexes in the melts depend on the total concentration of vanadium but does not depend on the type of alkali cation. At very low vanadium concentrations, $VO_2SO_4^-$ monomeric complexes are most probably formed. By increase of the vanadium concentration above $X_{V_2O_5} = 0.1$, association of the monomeric complexes takes place with the formation of dimeric $(VO)_2O(SO4)_4^{4-}$ and then oligomeric $(VO_2SO_4)_n^{n-}$ species. Further increase of the vanadium concentration diminishes the number of sulfate anions coordinated to vanadium. In pure vanadium (V) oxide, chains of VO_4 tetrahedra bridged by common oxygen atoms are retained in the melt.

The catalytic active species have been proposed to be a dimeric V(V) oxosulfato complex [20]. Indeed, recent investigations [21–23] of phase diagrams of the $M_2S_2O_7$–V_2O_5 systems (M=Na, K, Cs), XRD on isolated V(V) compounds [12], NMR measurements on melts [16] and high-temperature Raman spectroscopy [17,18] have shown that the dimeric V(V) complex $(VO)_2O(SO_4)_4^{4-}$ seems to dominate in the catalyst melt. The structure of this ion is shown in Fig. 2. The high-temperature Raman spectroscopic measurements [17,18] were carried out to establish the structural and vibrational properties of the vanadium complexes in the molten salt–gas system $M_2S_2O_7$–M_2SO_4–V_2O_5/SO_2–O_2–SO_3–N_2 (M=K, Cs) at 450°C and in the composition range

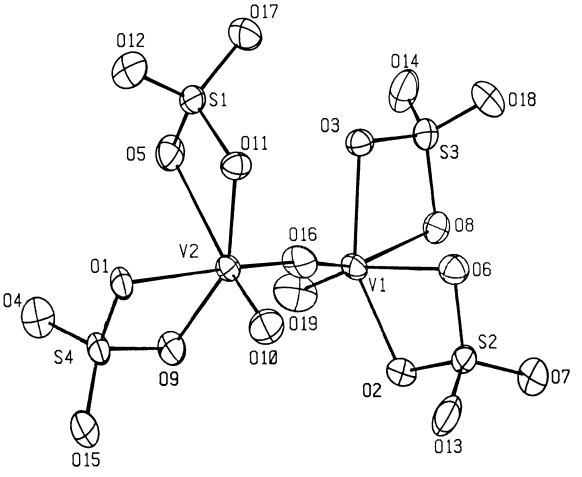

Fig. 2. Structure of the $(VO)_2O(SO_4)_4^{4-}$-ion [12].

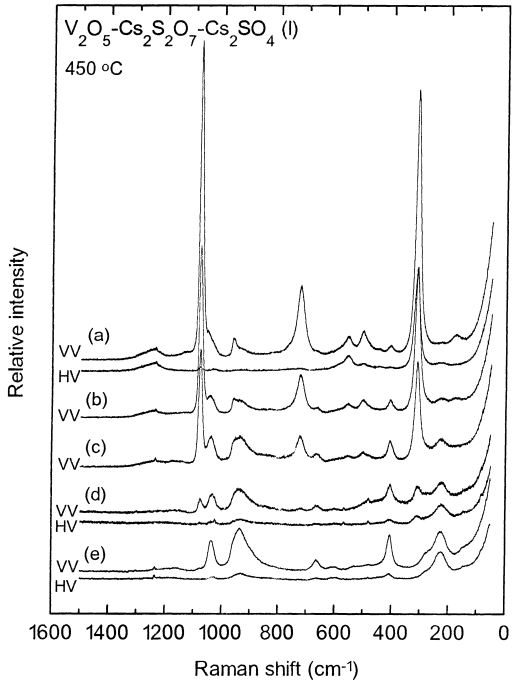

Fig. 3. Raman spectra of the $Cs_2S_2O_7$–V_2O_5 molten mixtures saturated with Cs_2SO_4 at 450°C. $X_{V_2O_5}$=0.027 (a), $X_{V_2O_5}$=0.066 (b), $X_{V_2O_5}$=0.147 (c), $X_{V_2O_5}$=0.330 (d). $X_{V_2O_5}$ in the mole fraction of V_2O_5 in the $Cs_2S_2O_7$–V_2O_5 mixture before addition of SO_4^{2-}. Raman spectra of the V_2O_5–$Cs_2S_2O_7$– $2Cs_2SO_4$ molten mixture at 450°C (e). λ_0=647.1 nm, laser power w=175 mW, scan rate 90 cm^{-1} min^{-1} for (a)–(c), 30 cm^{-1} min^{-1} for (d), 60 cm^{-1} min^{-1} for (e). Time constant, τ, 0.3 s for (a)–(c), 1 s for (d)–(e). Spectra slit width, sww, 7 cm^{-1}.

$X_{V_2O_5}$=0–0.25 (up to 4 mol V dm^{-3}), thus covering the catalytically important concentration range (usually in the range $X_{V_2O_5}$=0.18–0.22). This is the first time that high-temperature Raman spectra have been obtained on these very dark-colored, viscous and hygroscopic melts. Furthermore, proposals for the molecular structure of the V(V) complexes in the above catalyst model melts are presented, for the first time these being based on high-temperature vibrational spectroscopy.

The Raman spectral data for the $M_2S_2O_7$–V_2O_5 melts indicated that vanadium pentoxide reacts with molten alkali pyrosulfate to form an oxygen-bridged dimeric V(V) complex as follows:

$$V_2O_5 + 2S_2O_7^{2-} \rightarrow (VO)_2O(SO_4)_4^{4-} \quad (1)$$

whereas addition of M_2SO_4 to the $M_2S_2O_7$–V_2O_5 molten mixtures results – as judged from the Raman spectra – in alterations in the type of sulfate coordination and the structure of the V(V) complexes. A careful study of a titration-like series of Raman spectra showed that the V(V) dimer complex $[(VO)_2O(SO_4)_4^{4-}]$ reacted with the added sulfate up to an $SO_4^{2-}/V(V)$ ratio (ratio of number of added sulfate moles reacting vs. the number of extant V(V) atoms) equal to 1. Furthermore, the Raman spectra obtained for the M_2SO_4 molten mixtures, provided conclusive evidence that cleavage of the V–O–V bridge occurred upon sulfate addition. Fig. 3 shows a series of spectra obtained for $Cs_2S_2O_7$–V_2O_5 molten solutions with initial concentrations $X_{V_2O_5}$=0.03–0.50 in which various amounts of Cs_2SO_4 were added.

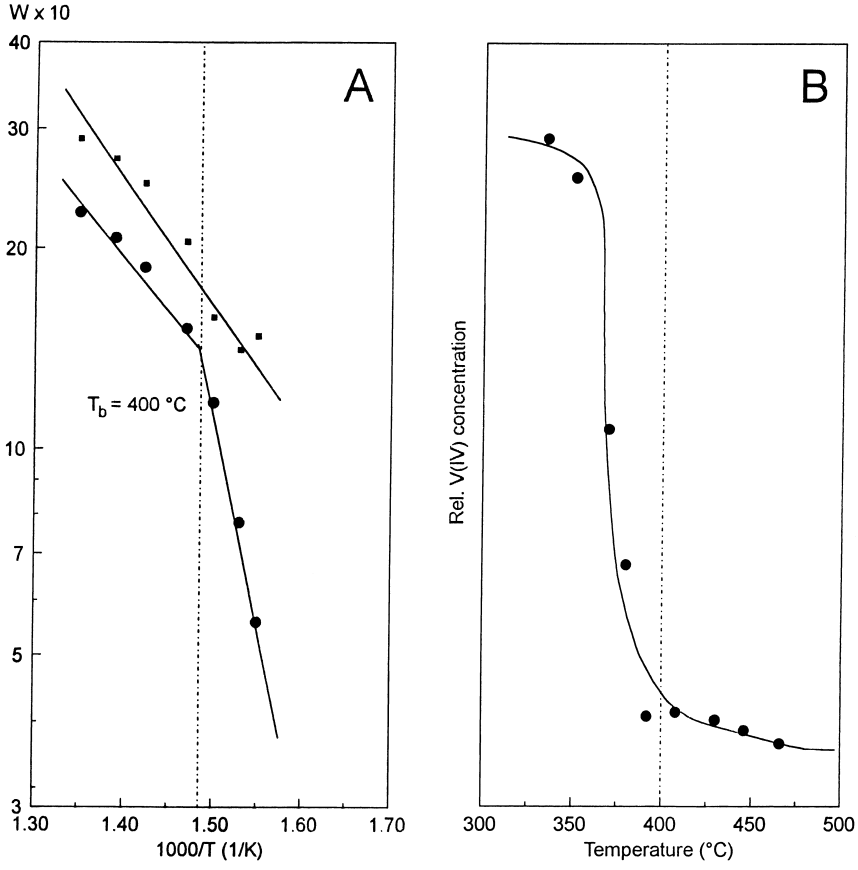

Fig. 4. (A) Lower curve: Arrhenius plots of VK-WSA referred to total vanadium content in 7.7% SO_3, 1.7% SO_2, 6.2% O_2 and 84.4% N_2 (82% preconversion). Upper curve: same plot but referred to vanadium in oxidation state (V) only. (B) Relative V(IV) concentration in VK-WSA vs. the temperature.

Spectrum (d) was obtained for a mixture with $X_{V_2O_5}$=0.33 saturated with Cs_2SO_4. The mole fraction $X_{V_2O_5}$ =0.33 corresponds to the stoichiometry of the $(VO)_2O(SO_4)_4^{4-}$ dimer complex. However, the observation of the band at 1078 cm^{-1} in spectrum (d) shows that $S_2O_7^{2-}$ was produced or (literally) was still present after saturation with the sulfate. The above observations of: (i) a 1:1 $SO_4^{2-}/V(V)$ ratio of the number of added sulfate moles reacting vs. the number of extant V(V) atoms; (ii) the cleavage of the V–O–V bridge and production of $S_2O_7^{2-}$ upon sulfate addition, can only be accounted for by the following reaction:

$$(VO)_2O(SO_4)_4^{4-} + 2SO_4^{2-} \rightleftarrows 2VO_2(SO_4)_2^{3-} + S_2O_7^{2-} \quad (2)$$

This is fully consistent with the well characterized activation of vanadium sulfuric acid catalysts by SO_3. Spectrum (e) was obtained for a $Cs_2S_2O_7$–V_2O_5 mixture with $X_{V_2O_5}$=0.50 to which Cs_2SO_4 had been added up to a 1:1 $SO_4^{2-}/V(V)$ ratio, this corresponding to an overall composition $V_2O_5 \cdot Cs_2S_2O_7 \cdot 2Cs_2SO_4$ and is assigned to the molten $Cs_3VO_2(SO_4)_2$ complex produced by the summation of reactions (1) and (2).

Reaction rates as a function of temperature have been measured for a number of industrial catalysts and for the silica-supported model melts. One example is shown in Fig. 4(A) for the industrial catalyst VK-WSA (Haldor Topsoe A/S, Denmark). The Arrhenius plot shows a marked break (T_b) below which the catalyst very rapidly looses the activity and the activation energy becomes very high. Similar treatment of model catalyst melts in the molten salt reactor [11,24] cell leads to precipitation of V(IV) and/or V(III) compounds below the break point temperature as will be discussed below. Simultaneously with the activity measurements, in situ ESR spectra on the working VK-WSA catalyst have been recorded as shown in Fig. 5. Above 400°C the spectra reveal a broad line with unresolved hyperfine structure which is probably due to the presence of polymeric V(IV) species in solution, e.g. $[VO(SO_4)_2]_n^{2n-}$. In addition to the broad line, a rather weak 8-line feature seems to be present, indicating monomeric V(IV) complexes, such as $VO(SO_4)_2^{2-}$, in low concentration in the catalyst. Below 400°C, a sharp central anisotropic line dominates increasingly with further decrease of the temperature. This line has ESR parameters close to those found for β-$VOSO_4$, i.e. $g_\perp$=1.973 and $g_{||}$=1.920.

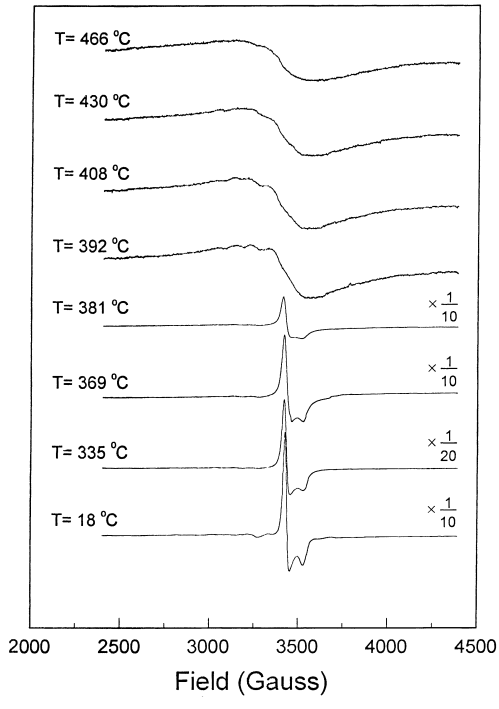

Fig. 5. In situ ESR spectra of VK-WSA in 7.7% SO_3, 1.7% SO_2, 6.2% O_2 and 84.4% N_2 ((82% preconversion) at different temperatures. For clarity some spectra are reduced by the indicated factor.

Thus, precipitation of β-$VOSO_4$ seems to deplete the melt of active vanadium species, leading to catalyst deactivation. Integration of the ESR spectra lead to the plot shown in Fig. 4(B) for the relative V(IV) concentration in the catalysts. A sharp increase in the V(IV) concentration (sum of dissolved and precipitated V(IV)) is observed below 400°C, the temperature of deactivation. Assuming that all the V(V) is reduced to V(IV) at 335°C, it is possible to calculate the actual concentration of V(V) at the different temperatures. Relating the measured activity only to the V(V) concentration leads to the plot shown in Fig. 4(A), a so-called Boreskov Plot, acknowledging the first paper [25] where such a plot was presented. It is seen that the break disappears indicating that the rate limiting step involves only V(V) species.

Recent investigations [26] of the catalysts VK38 (K, Na), VK58 (K, Na, Cs) and VK-WSA (Na, K) from Haldor Topsoe A/S (with the type of promoter given in parenthesis) using dry and wet simulated power plant

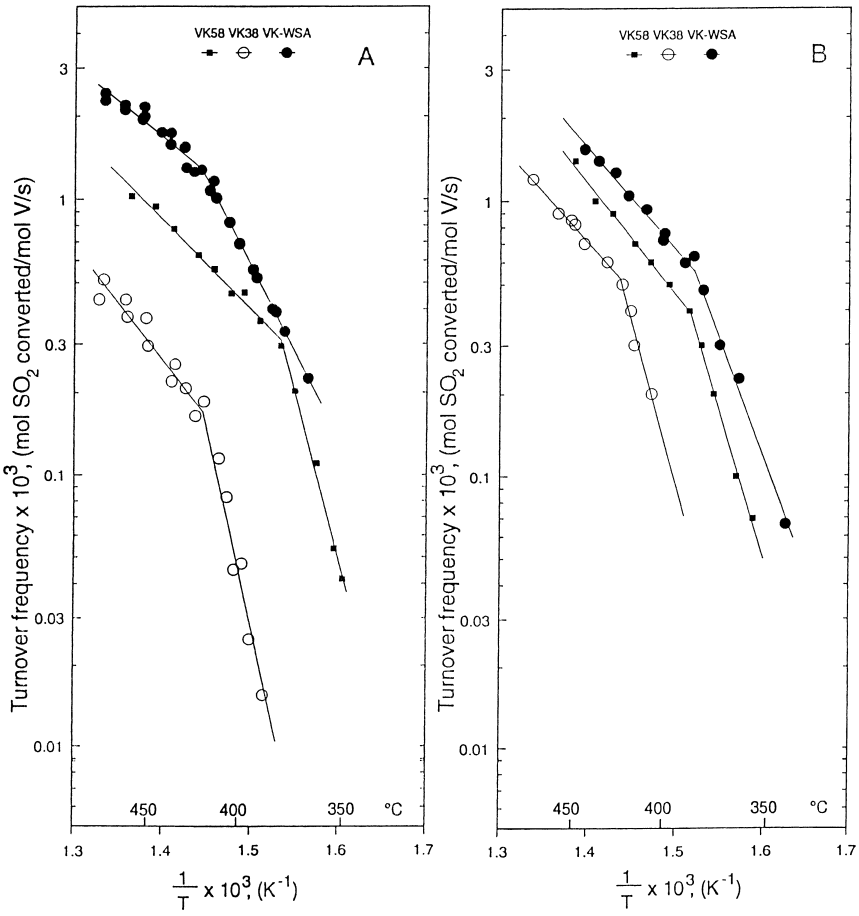

Fig. 6. Arrhenius plots of industrial sulfuric acid catalysts in (A) 0.2% SO_2 4.5% O_2, 15.1% CO_2 and 80.2% N_2 (dry flue gas) and (B) 0.2% SO_2, 4% O_2, 7% H_2O, 14% CO_2 and 74.8% N_2 (wet flue gas).

flue gases has shown (Fig. 6) similar breaks in the Arrhenius plots. The Cs-promoted catalyst exhibited the lowest temperature of deactivation in the dry flue gas and the VK-WSA sample showed a remarkable improvement in the low temperature activity in the wet flue gas. The simultaneously recorded ESR spectra of the catalysts showed good accordance between the break point temperature, T_b, and the temperature of precipitation, T_p, except for VK-WSA in the wet gas, as shown in Fig. 7. Here the plot of the ESR line width shows no break and the features of the ESR spectrum give no evidence of a V(IV) compound precipitating above ~350°C. Fig. 8 shows the results from a double integration of the ESR spectra in dry and wet flue gas (two runs). In the dry gas (Fig. 8(A)), there is a good agreement between T_b and T_p, and the steep rise in V(IV) concentration below T_b is caused by the precipitation at T_b of the V(IV) compound $K_4(VO_3)(SO_4)_5$, judged from the ESR parameters of the sharp central line (Fig. 7(A)).

In the wet gas, however, a maximum of the V(IV) concentration seems to be found close to T_b (Fig. 8(B)). This is explained by the precipitation of an ESR-silent V(III) compound which, according to the linked complex equilibrium V(III)⇄V(IV)⇄V(V), will reduce the concentration of V(IV) and V(V) in the solution when it starts to precipitate at T_b. At T_p, a V(IV) compound also precipitates, as judged from the ESR spectra (not indicated in Fig. 7(B)). Earlier [11] it has indeed been shown that both V(III) and V(IV) compounds might precipitate in the model catalyst melts.

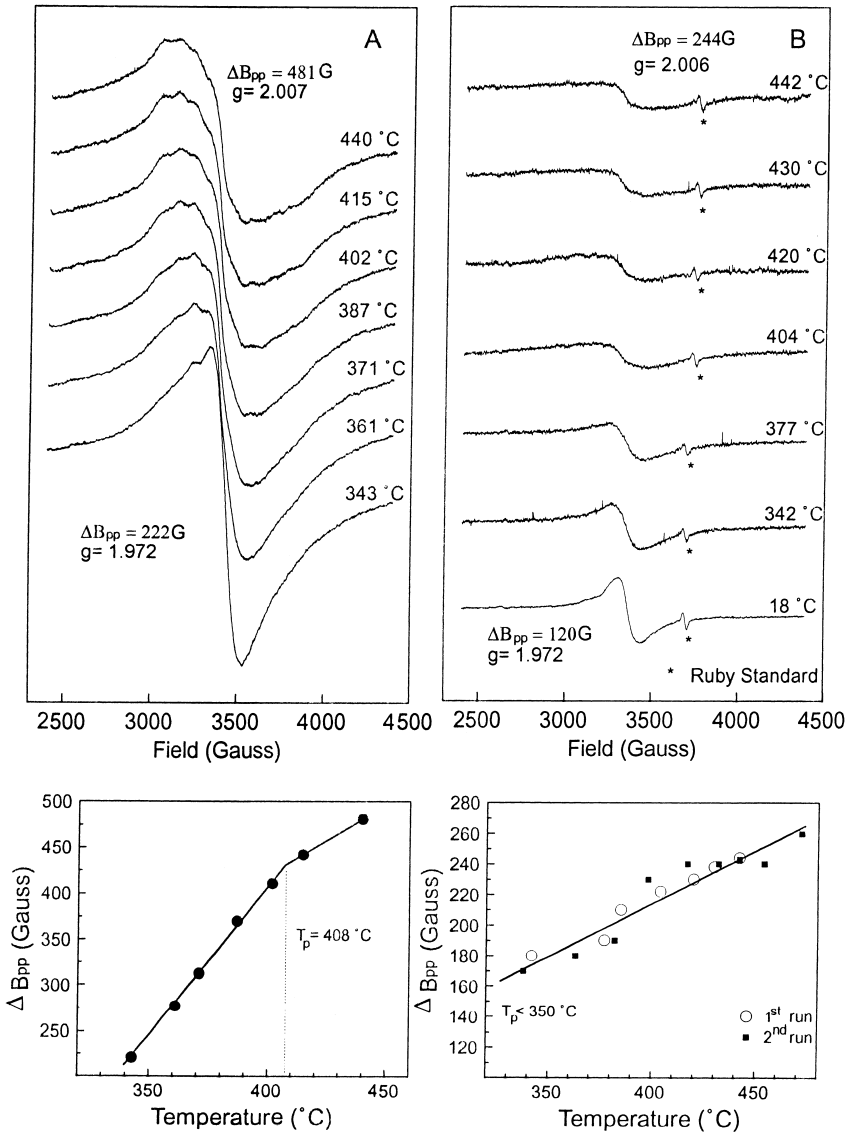

Fig. 7. In situ ESR spectra of VK-WSA at various temperatures in (A) 0.2%SO_2, 4.5% O_2, 15.1% CO_2 and 80.2% N_2 (dry flue gas) and (B) 0.2% SO_2, 4% O_2, 7% H_2O, 14% CO_2 and 74.8% N_2 (wet flue gas). Insert: apparent line width (ΔB_{pp}) vs. temperature. The dotted line represents the temperature T_p where a marked change in the linear relationship is observed.

Quantitatively, this observation can be explained by a marked difference in the concentration and solubility of the V(III) and V(IV) compounds as a function of temperature, as shown in Fig. 9. Usually the V(IV) concentration exceeds the solubility at T_b (dashed curve) at higher temperature, thus causing a V(IV) concentration profile as observed in Fig. 4(B) and Fig. 8(A). However, for VK-WSA in the wet flue gas, the V(III) concentration probably exceeds the solubility at T_b, thus causing the scenario in Fig. 9 indicated by the dotted curves. This is qualitatively in agreement with the V(IV) concentration profile in Fig. 8(B). The catalyst VK-WSA has smaller pores than VK38 and VK58. This probably suppresses the growth of V(IV) crystalline compounds but not that of V(III) to the same extent.

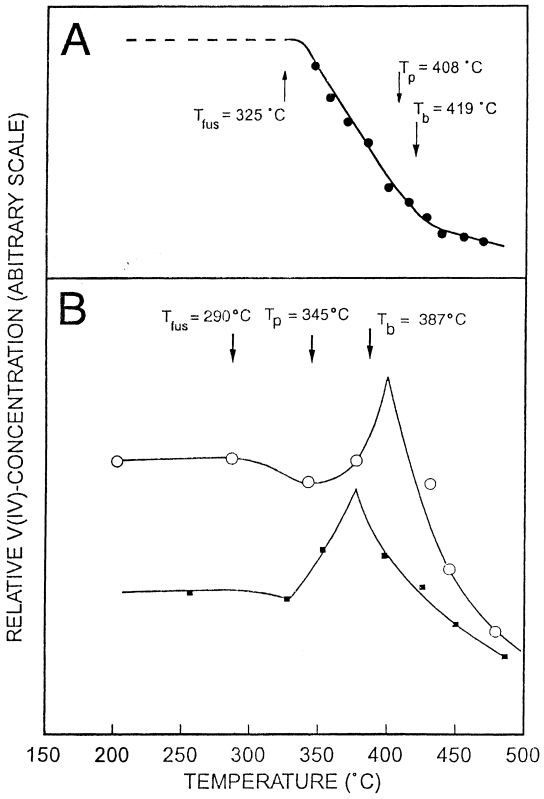

Fig. 8. Relative V(IV) concentration vs. temperature for VK-WSA in (A) dry flue gas and (B) wet flue gas (two runs). Constant level indicates the solidification temperature of the catalyst. The break point temperatures (T_b) and temperature of precipitation (T_p) are indicated.

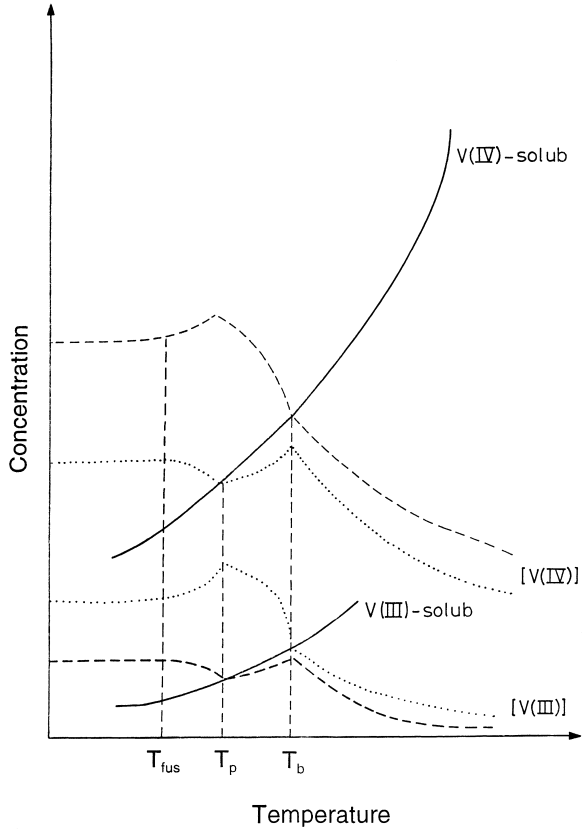

Fig. 9. Qualitative diagram of possible concentration and solubility curves for V(III) and V(IV) vs. temperature for VK-WSA in flue gas. Dashed and dotted curves indicate alternative scenarios for crystalline compound precipitation.

Thus, much evidence shows that the catalyst melt is depleted with respect to the active vanadium species below the break point temperature of the Arrhenius activity plots, thus leading to catalyst deactivation. Table 1 summarises the type and compositions of the compounds isolated from the catalyst model melts during deactivation. The compounds have been characterized by XRD and spectroscopic methods, as described recently [24]. Based on the ESR spectra of the compounds, the in situ ESR investigations on working industrial catalysts indeed reveal that similar compounds are formed in the catalysts during deactivation.

It is important to notice that the types of compound precipitating also depend on the composition of the gas mixture. Thus, the compound $K_4(VO)_3(SO_4)_5$ contains more sulfate per vanadium atom than does β-$VOSO_4$. This is in accordance with the higher partial pressure of SO_3 found when β-$VOSO_4$ precipitates: the melt equilibrium $SO_4^{2-} + SO_3 \rightleftarrows S_2O_7^{2-}$ will

Table 1
Possible compounds responsible for catalyst deactivation

V(IV)	V(III)
$Na_2VO(SO_4)_2$	$NaV(SO_4)_2$
$Na_3(VO)_2(SO_4)_4$[a]	$Na_3V(SO_4)_3$
$K_4(VO)_3(SO_4)_5$	$KV(SO_4)_2$
$K_3(VO)_2(SO_4)_4$[a]	
$Cs_2(CO)_2(SO_4)_3$	$CsV(SO_4)_2$
β-$VOSO_4$	
$VOSO_4(SO_2SO_3)x$[b]	

[a] Mixed valence V(IV)–V(V) compounds.
[b] $VOSO_4$ – like lattice with incorporated SO_2 and/or SO_3 molecules.

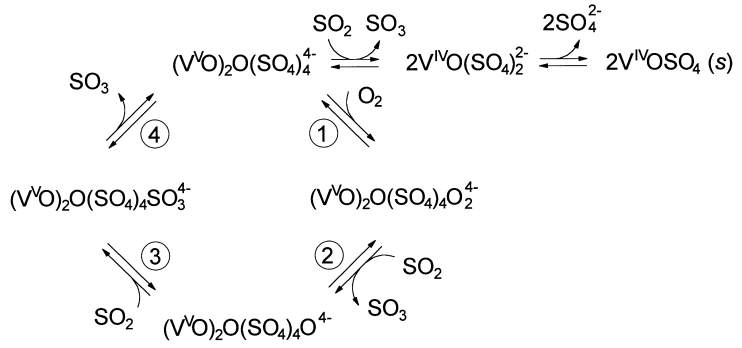

Fig. 10. Proposal for the reaction mechanism of SO_2 oxidation.

accordingly be shifted to a lower sulfate activity in the melt.

Very recently [27] modeling of the crystallization process in Russian catalysts by Monte Carlo calculations combined with ESR measurements has supported the conclusion that catalyst deactivation is indeed caused by precipitation of V(IV) compounds. Furthermore, it has been found that the pore size of the catalyst support is an important parameter in relation to the temperature of deactivation.

4. Conclusions

From the combined results, a new and more detailed mechanism for the vanadium catalyzed oxidation of SO_2 can be suggested, as shown in Fig. 10. The catalytic cycle involves only V(V) species (dimeric or binuclear fragments of larger oligomers [20]), while a side reaction leads to reduction of V(V) to the catalytically inactive V(IV) (or V(III)) as shown in Fig. 10, where the precipitating compound is depicted by $VOSO_4$. The bidentate ligands found within the dimeric $[(VO)_2O(SO_4)_4]^{4-}$ complex are strained due to their unusually large distortion. Some of these sulfate ligands may open up, making the complex coordinatively unsaturated in the horizontal positions and leading to the suggested coordination of O_2 shown in Fig. 10, step 1. The O_2 in this complex is activated for the reaction with SO_2, steps 2 and 3, activation of O_2 in the coordination sphere of transition metals being a well known phenomenon [28]. In step 4, SO_3 is eliminated and the unsaturated dimeric species is reformed. Attempts to characterize the suggested complexes are in progress.

Acknowledgements

INTAS (Contract no. 93-3244 and 93-3244 Ext.), RFBR (Grant 95-03-08365a) and several other EU programs and national research foundations have supported the present work.

References

[1] G.K. Boreskov. Catalysis in Sulphuric Acid Production, Goskhimizdat (in Russian), Moskow, 1954, p. 348.
[2] J.H. Frazer, W.J. Kirkpatrick, J. Am. Chem. Soc. 62 (1940) 1659.
[3] H.F.A. Topsoe, A. Nielsen, Trans. Dan. Acad. Tech. Sci. 1 (1947) 18.
[4] J. Villadsen, H. Livbjerg, Catal. Rev.-Sci. Eng. 17 (1978) 203.
[5] C.N. Kenney, Catal. Rev.-Sci. Eng. 11 (1975) 197.
[6] O.B. Lapina, V.M. Mastikhin, A.A. Shubin, V.N. Krasilnikov, K.I. Zamaraev, Progr. NMR spectrosc. 24 (1992) 457.
[7] V.M. Mastikhin, O.B. Lapina, Vanadium catalysts: solid state NMR, in: Encyclopedia of Nuclear Magnetic Resonance, vol. 8, Wiley, 1996, p. 4892.
[8] G.K. Boreskov, L.P. Davydova, V.M. Mastikhin, G.N. Polyakova, Dokl. Akad. Nauk SSSR, Ser. Khim. (in Russian) 171 (1966) 648.
[9] V.M. Mastikhin, G.N. Polyakova, J. Ziolkowsky, G.K. Boreskov, Kinet. Katal. (in Russian) 1 (1970) 1463.
[10] S.V. Kozyrev, B.S. Bal'zhinimaev, G.K. Boreskov, A.A. Ivanov, V.M. Mastikhin, React. Kinet. Catal. Lett. 20 (1982) 53.
[11] S. Boghosian, R. Fehrmann, N.J. Bjerrum, G.N. Papatheodorou, J. Catal. 119 (1989) 121 and references therein.

[12] A. Nielsen, R. Fehrmann, K.M. Eriksen, Inorg. Chem. 32 (1993) 4825 and references therein.
[13] D.A. Karydis, K.M. Eriksen, R. Fehrmann, S. Boghosian, J. Chem. Soc., Dalton Trans. 2151 (1994) and references therein.
[14] K.M. Eriksen, R. Fehrmann, G. Hatem, M. Gaune-Escard, O.B. Lapina, V.M. Mastikhin, J. Phys. Chem. 100 (1996) 10771 and references therein.
[15] K.M. Eriksen, R. Fehrmann, N.J. Bjerrum, J. Catal. 132 (1991) 263.
[16] O.B. Lapina, V.M. Mastikhin, A.A. Shubin, K.M. Eriksen, R. Fehrmann, J. Mol. Catal. A 99 (1995) 123.
[17] S. Boghosian, A. Chrissanthopoulos, F. Borup, Catal. Lett. 48 (1997) 145.
[18] A. Chrissanthopoulos, F. Borup, R. Fehrmann, S. Boghosian, to be submitted.
[19] S. Boghosian, G.N. Papatheodorou, J. Phys. Chem. 93 (1989) 415.
[20] B.S. Bal'zhinimaev, A.A. Ivanov, O.B. Lapina, V.M. Mastikhin, K.I. Zamaraev, Faraday Discuss. Chem. Soc. 87 (1989) 133.
[21] D.A. Karydis, S. Boghosian, R. Fehrmann, J. Catal. 145 (1994) 312.
[22] G.E. Folkmann, G. Hatem, R. Fehrmann, M. Gaune-Escard, N.J. Bjerrum, Inorg. Chem. 30 (1991) 4057.
[23] G.E. Folkmann, K.M. Eriksen, R. Fehrmann, G. Hatem, M. Gaune-Escard, O.B. Lapina, V. Terskikh, J. Phys. Chem. B 102 (1998) 24.
[24] K.M. Eriksen, D.A. Karydis, S. Boghosian, R. Fehrmann, J. Catal. 155 (1995) 321 and references therein.
[25] G.K. Boreskov, G.N. Polyakova, A.A. Ivanov, V.M. Mastikhin, Dokl. Akad. Nauk SSSR, Ser. Khim. (in Russian) 210 (1973) 626.
[26] S.G. Masters, A. Chrissanthopoulos, K.M. Eriksen, S. Boghosian, R. Fehrmann, J. Catal. 166 (1997) 16.
[27] C. Oehlers, R. Fehrmann, S.G. Masters, K.M. Eriksen, D.E. Sheinin, B.S. Balzhinimaev, V.I. Elokhin, Appl. Catal. 147(1) (1996) 127.
[28] J.S. Valentine, Chem. Rev. 73(3) (1973) 235.